Phase transition of maize starch in aqueous ionic liquids: Effects of water:ionic liquid ratio and cation alkyl chain length

Fei Ren[a, b], Fengwei Xie[c,d], Huiyu Luan[ab], Shuo Wang[e], Shujun Wang*[a, b]

[a] State Key Laboratory of Food Nutrition and Safety, Tianjin University of Science & Technology, Tianjin 300457, China

[b] School of Food Science and Technology, Tianjin University of Science & Technology, 300457, China

[c] International Institute for Nanocomposites Manufacturing (IINM), WMG, University of Warwick, Coventry CV4 7AL, United Kingdom

[d] School of Chemical Engineering, The University of Queensland, Brisbane, Qld 4072, Australia

[e] Tianjin Key Laboratory of Food Science and Health, School of Medicine, Nankai University, Tianjin 300071, China

*** Corresponding authors:** Dr. Shujun Wang

Mailing address: No 29, 13th Avenue, Tianjin Economic and Developmental Area (TEDA), Tianjin 300457, China

Phone: 86-22-60912486

E-mail address: sjwang@tust.edu.cn

Abstract: The thermal phase transition behavior of maize starch in water:ionic liquid (IL) mixtures was investigated. With decreasing water:IL molar ratio to 10:1, the endothermic transition shifted to higher temperatures, and then to lower temperatures at 5:1 water:IL ratio. At 2:1 water:IL ratio, an exothermic transition occurred at a lower temperature than gelatinization temperature of starch in pure water. At the same water:IL ratios (35:1 to 5:1), the endothermic transition temperatures of starch increased with decreasing alkyl chain length of the cation, whereas an opposite trend was found for the exothermic transition at 2:1 water:IL ratio. Rheological, ^{1}H NMR and FTIR analyses of water:IL mixtures showed that with decreasing water:IL ratio, the viscosity of water:IL mixture and the interactions between cation and anion increased, whereas the interactions between IL and water increased and then decreased. The endothermic transition of starch in water:IL mixtures of 35:1 to 5:1 was affected by the water availability for gelatinization. However, the exothermic transition of starch in water:IL mixtures of 2:1 was mainly caused by the interactions between IL and starch and viscosity of water:IL mixtures.

Keywords: starch phase transition; ionic liquid-water mixture; water availability; alkyl chain length; molecular interactions.

Abbreviations: MS, maize starch; [C_4mim][Cl], 1-butyl-3-methylimidazolium chloride; [C_3mim][Cl], 1-propyl-3-methylimidazolium chloride; [C_2mim][Cl], 1-ethyl-3-methylimidazolium chloride; T_o, onset temperature; T_p, peak temperature; T_c,

conclusion temperature; ΔH, enthalpy change.

1. Introduction

With the imminent depletion of petroleum resources and increased environmental pollution, the use of renewable resources especially biopolymers (e.g., cellulose, starch, chitin, chitosan, and lignin) to replace synthetic polymers for the manufacture of green materials has received much attention (Mahmood et al., 2017b). However, the presence of strong inter- and intra-molecular hydrogen bonds in biopolymers makes them difficult to dissolve in many conventional solvents, thus limiting the processing of these biopolymers (Mekonnen et al., 2013). Recently, ionic liquids (ILs) are used as "green solvents" in the fabrication of biodegradable materials because of their unique properties such as negligible vapor pressure, non-flammability, and high chemical and thermal stability (Mäki-Arvela et al., 2010; Zhu et al., 2006). ILs are defined as salts with low melting point (< 100 °C), consisting of an organic cation and an organic or inorganic anion (Egorova et al., 2017). ILs made up of a chloride anion and an imidazolium cation are found to be effective at dissolving biopolymers (Pinkert et al., 2009). However, pure ILs have some disadvantages in the dissolution of biopolymers such as high cost, viscosity and processing temperature (typically over 100 °C). To overcome these issues, the mixtures of ILs with other solvents (e.g., water (Xu et al., 2017; Zhang et al., 2017a), *N*,*N*-dimethylformamide (Xu et al., 2015a) and *N*,*N*-dimethylacetamide (Xu et al., 2015b)) have been used to dissolve biopolymers at ambient temperature.

Among renewable biopolymers investigated as potential alternatives to traditional petroleum-based polymers, starch has gained huge interest due to its wide availability, biodegradability, and regeneration (Shogren et al., 1993). Starch often undergoes gelatinization, dissolution or plasticization in the presence of water or other plasticizers during processing. Although the starch structure is disrupted during processing, the granule remnants may still be present (Debet and Gidley, 2007). The incomplete dissolution or plasticization of starch represents an issue when trying to obtain homogeneous amorphous materials. Recently, aqueous ILs have been used as an effective solvent for starch dissolution and plasticization (Wilpiszewska and Spychaj, 2011), facilitating the development of starch-based materials, such as thermoplastic starch (Decaen et al., 2017; Mahmood et al., 2017a; Sankri et al., 2010), solid polymer electrolytes (Ning et al., 2009; Ramesh et al., 2011), and starch-based conducting films (Xie et al., 2015; Zhang et al., 2017b).

The understanding of the phase transition of starch is crucial to the development of emerging biodegradable starch-based materials. Over the past few years, the starch phase transition in water:IL mixtures have been paid much attention due to the application of ILs or their aqueous solutions in the processing of starch. With increasing IL concentration in water, the phase transition of starch was observed to change from a single endotherm, to a endotherm plus an exotherm, and finally to only a single exotherm (Mateyawa et al., 2013; Sciarini et al., 2015; Xiang et al., 2018;

89 Zhang et al., 2016; Zhao et al., 2015). By characterizing the structural changes of
90 starch during phase transition, the mechanisms underlying the endotherm and
91 exotherm of starch in water:IL mixtures were revealed (Xiang et al., 2018). The phase
92 transition behavior of starch in water:IL mixtures was assumed to be affected by the
93 viscosity of the water:IL mixtures and the interactions between ILs and water (Liu and
94 Budtova, 2013; Zhang et al., 2015). However, this assumption has not been verified
95 and needs to be supported by further evidence.
96
97 On the other hand, although the cationic structure of ILs can greatly affect the
98 interactions between IL and water (Papanyan et al., 2013; Ren et al., 2019;
99 Vicent-Luna et al., 2017) and between IL and biopolymer (Lappalainen et al., 2013;
100 Lu et al., 2014; Ren et al., 2019; Xu et al., 2018), there have been limited studies on
101 the effect of the cationic moiety of ILs on the phase transition behavior of starch in
102 water:IL mixtures. Hence, the aim of the present study is to investigate the effect of
103 the alkyl chain length of the imidazolium cation and water:IL ratios on the phase
104 transition of maize starch using differential scanning calorimetry (DSC) and light
105 microscopy. To better understand phase transition of starch in aqueous IL solutions,
106 the properties of water:IL mixtures were investigated by rheology, attenuated total
107 reflectance-Fourier transform infrared (ATR-FTIR) spectroscopy, and nuclear
108 magnetic resonance (NMR) spectroscopy.
109
110 **2. Materials and methods**

2.1. Materials

Normal maize starch (10.1% moisture and 22.4% amylose contents) was purchased from Sigma Chemical Co. (St. Louis, MO, USA). The ILs (1-butyl-3-methylimidazolium chloride, [C_4mim][Cl]; 1-propyl-3-methylimidazolium chloride, [C_3mim][Cl]; 1-ethyl-3-methylimidazolium chloride, [C_2mim][Cl]) were supplied by Nuowei Chemistry Co., Ltd. (Wuhu, Anhui, China) and used without further purification. According to the supplier, the purity of these ILs was all ≥ 95 weight% (water content < 0.5 weight%). The chemical structures of these imidazolium-based ILs are depicted in Figure 1. Milli-Q water was used in all instances. The water:IL mixtures with different water:IL molar ratios (35:1, 15:1, 10:1, 5:1 and 2:1) were prepared at ambient temperature (25±0.5 °C). In this article, the abbreviation "water:IL-n:m-MS" is used subsequently to indicate that the maize starch (MS) was heated in the water:IL mixtures at the molar ratio of n:m.

2.2. Differential scanning calorimetry

Differential scanning calorimetry (DSC) measurements were performed using a differential scanning calorimeter (200F3, Netzsch, Germany) equipped with a thermal analysis data station. For each measurement, approximately 3 mg of the native starch was weighed into an aluminum pan and 9 mg of a certain water:IL mixture were added to obtain a starch/aqueous IL ratio of 1:3 (weight/weight) (Xiang et al., 2018). The pans were shaken gently to ensure complete immersion of the starch in the liquid before sealing the pans. The DSC profiles were recorded immediately. The pans were

heated from 20 to 100 °C at a heating rate of 10 °C min^{-1}. An empty aluminum pan was used as the reference. The onset (T_o), peak (T_p), conclusion (T_c) temperatures and the enthalpy change of phase transition (ΔH) were recorded. When a water:IL ratio of 5:1 was used, the thermogram was more complex. In this case, four temperatures were defined and determined: T_o is defined as the onset temperature of the initial exotherm; T_c means the conclusion temperature of the subsequent endotherm; T_{p1} represents the peak temperature of the exotherm; and T_{p2} indicates peak temperature of the endotherm.

2.3. Light microscopy

A light microscope with a hot-stage thermosystem (DM-4000M-LED, Leica, Germany) was used. Starch suspensions (0.5 wt%) in water:IL mixtures were prepared in glass vials (Mateyawa et al., 2013). A drop of the starch suspension was transferred onto a glass slide, which was covered by another glass slide. Silicon adhesive was used to seal the starch suspension between the two glass slides to avoid moisture evaporation during observation. Starch samples were heated from 25 °C to 100 °C at a rate of 2 °C min^{-1}, and the images at T_o, T_p and T_c (obtained from DSC) were captured.

2.4. Rheology

Rheological measurements of water:IL mixtures were performed on an Anton Paar MCR302 rheometer (Anton Paar, GmbH., Austria) with a Peltier temperature control

155 system. The measuring system has a cone-plate geometry with 4° angle and 40 mm
156 diameter (Hall et al., 2012). For each solution, the steady-shear viscosity was recorded
157 as a function of shear rate from 10 s^{-1} to 500 s^{-1} at a constant temperature (25 °C).
158 Silicone oil was placed around the edge of the measuring cell to prevent water vapor
159 absorption and evaporation.
160
161 **2.5. Attenuated total reflectance Fourier-transform infrared (ATR-FTIR)**
162 **spectroscopy**
163 ATR-FTIR spectra of water:IL mixtures were obtained using a Thermo Scientific
164 Nicolet IS50 spectrometer (Thermo Fisher Scientific, USA). Approximately 50 μL of
165 water:IL mixtures was scanned from 4000 to 400 cm^{-1} at ambient temperature (Zhang
166 et al., 2015). The spectra were obtained at a resolution of 4 cm^{-1} with an accumulation
167 of 32 scans against the air as the background.
168
169 **2.6. Nuclear magnetic resonance (NMR) spectroscopy**
170 Mixtures of D_2O:IL at different molar ratios (35:1, 15:1, 10:1, 5:1 and 2:1) were
171 prepared for NMR measurement. ^1H NMR spectra of D_2O:IL mixtures were obtained
172 using a DMX 300 NMR spectrometer (300 MHz) (Bruker, Germany) at ambient
173 temperature (Chen et al., 2014).
174
175 **2.7. Statistical analysis**
176 All analyses were performed at least in triplicate and the results are reported as mean

177 value plus standard deviation. For ATR-FTIR and ^{1}H NMR, only one measurement
178 was performed. One-way analysis of variance (ANOVA) followed by post-hoc
179 Duncan's multiple range tests ($p < 0.05$) was conducted to determine the significant
180 differences between mean values using SPSS 17.0 Statistical Software (SPSS Inc.
181 Chicago, IL, USA).
182
183 **3. Results and discussion**
184 **3.1. Thermal properties of starch in water:IL mixtures**
185 Figure 2 shows the DSC thermograms of native maize starch in water:IL mixtures and
186 the corresponding thermal transition parameters are listed in Table 1. During DSC
187 heating, a single well-defined gelatinization endotherm was observed between 65.8 °C
188 and 76.9 °C for the native starch in pure water. For each type of ILs, the phase
189 transition was changed from only a single endotherm to a small exotherm followed by
190 an endotherm (at water:IL ratio of 5:1), and then to a single exotherm with decreasing
191 water:IL ratio to 2:1. These transitions were attributed to the gelatinization transition
192 of starch, except the small exotherm observed at low temperatures for starch at a
193 water:IL ratio of 5:1, which was explained as being due to the interaction between
194 amorphous starch and IL rather than the melting of starch crystallites (Xiang et al.,
195 2018).
196
197 With decreasing water:IL ratio to 15:1, the single endothermic transition shifted to
198 higher temperatures. A further decrease in water:IL ratio to 10:1 did not result in a

significant shift of the endotherm ($p > 0.05$). At a water:IL ratio of 5:1, the endothermic transition shifted to lower temperatures. When the water:IL ratio was 2:1, the single exotherm occurred at a temperature lower than the gelatinization temperatures of the starch-water system. The enthalpy change (ΔH) increased with decreasing water:IL ratio to 10:1, and then decreased for 5:1 water:IL ratio. At 2:1 water:IL ratio, the only wide exothermic transition had ΔH of −5.7 to −10.5 J/g ($p < 0.05$). These observations indicate that the addition of ILs to water delayed the progression of starch gelatinization at water:IL ratios of 35:1, 15:1, 10:1 and 5:1, but facilitated such transition at a lower water:IL ratio of 2:1.

At water:IL ratios of 35:1, 15:1, 10:1 and 5:1, T_o, T_p, T_c and ΔH of the endotherm for the starch gelatinization followed the order $[C_2mim][Cl]$ > $[C_3mim][Cl]$ > $[C_4mim][Cl]$. At 2:1 water:IL ratio, the exothermic transition temperatures decreased, and the exothermic enthalpy increased from 5.7 J/g to 10.5 J/g with decreasing cation alkyl chain length from C4 to C2. These results suggest that a longer cation alkyl chain length facilitated the starch gelatinization at high water:IL ratios (between 35:1 and 5:1), but delayed the starch gelatinization at lower water:IL ratio of 2:1.

3.2. Morphological changes of starch granules during phase transition in water:IL mixtures

Figure 3 shows the light and polarized light microscopic images of native maize starch in pure water and water:IL mixtures during heating. Similar granule

morphology was observed for the starch in three different types of water:IL mixtures, thus only the images of water:[C_4mim][Cl]-MS are shown here. The native starch presented a well-defined granule structure and clear birefringent (Maltese cross) patterns (Figure 3, a1 and a2). Whether being heated in pure water or water:IL mixtures of 35:1 to 10:1, the starch showed similar changes in granule morphology. Upon heating to T_o of the gelatinization endotherm, the starch granules remained intact with clear birefringent patterns (Figure 3, b1, b4, c1 and c4), although the brightness of Maltese cross patterns became weaker compared with that of the native starch. This observation was consistent with the previous finding that starch gelatinization is initiated earlier than T_o of the endotherm (Jenkins and Donald, 1998; Liu et al., 2019; Ratnayake et al., 2009). At T_p of gelatinization endotherm, most of the granules were greatly swollen and deformed with less remaining birefringence (Figure 3, b2, b5, c2 and c5). Starch granules were completely disrupted with no birefringence at T_c (Figure 3, b3, b6, c3 and c6). As the water:IL ratio decreased to 5:1, there was no apparent change in the granule morphology at T_o and T_{p1} of the exotherm (Figure 3, d1, d2, d5 and d6), whereas all granules were destroyed with no birefringence at T_{p2} of endotherm (Figure 3, d3 and d7). It is interesting to note that at T_p of the exothermic transition for the 2:1 water:IL mixture, most granules were still intact and showed birefringence (Figure 3, e2 and e5), although no granule remnants and birefringence were observed at T_c (Figure 3, e3 and e6).

3.3. Rheological properties of water:IL mixtures

The steady-shear viscosities of pure water and water:IL mixtures are compared (Table 2). Viscosity increased with decreasing water content in the water:IL mixtures and with increasing alkyl chain length of the IL cation, which is in general agreement with our previous results (Ren et al., 2019). While the 35:1, 15:1 and 10:1 water:IL mixtures all exhibited a low viscosity (< 4.0 mPa·s), further increases in IL concentration led to the significantly increased viscosity of water:IL mixtures (p < 0.05). Irrespective of the IL type, the viscosities of 5:1 water:IL mixtures were about twice those of 10:1 water:IL mixtures; and the viscosities of 2:1 water:IL mixtures were 3-4 times those of the 5:1 mixtures.

3.4. ATR-FTIR analysis of water:IL mixtures

Figure 4 shows the ATR-FTIR spectra of pure water and different water:IL mixtures and the wavenumbers representing the -OH stretching mode of water (3000-3800 cm^{-1}) (Cammarata et al., 2001) are listed in Table 2. The band in this region was observed to shift to higher wavenumbers after mixing water with an IL, indicative of the interactions occurring between water and the IL. This blue shift increased with decreasing water:IL ratio to 10:1, but decreased with further increasing water:IL ratio to 2:1. This indicates that the interactions between the IL and water gradually increased to a maximum and then decreased as the water:IL ratio was decreased. At the same water:IL ratio, the -OH stretching band shifted to higher wavenumbers with increasing alkyl chain length of the IL cation, indicating that the interactions between water and ILs with longer alkyl chain were stronger.

265

266 **3.5. ^{1}H NMR analysis of water:IL mixtures**

267 The ^{1}H-NMR spectra of water:IL mixtures are shown in Figure 5 and the chemical
268 shifts of hydrogens tethered at carbons C(2), C(4) and C(5) on the imidazolium ring
269 (designated as $\delta_{H(2)}$, $\delta_{H(4)}$ and $\delta_{H(5)}$, respectively) are listed in Table 2. The changes in
270 the chemical shift of these hydrogens are indicative of interactions between cation and
271 anion or between cation and water molecules (Chen et al., 2014). With decreasing
272 water:IL ratio from 35:1 to 2:1, $\delta_{H(2)}$, $\delta_{H(4)}$ and $\delta_{H(5)}$ increased gradually, indicating the
273 increased aggregation of IL ion pairs enhancing the cation-anion interactions (Chen et
274 al., 2014; Hall et al., 2012; Ren et al., 2019; Vicent-Luna et al., 2017). At the same
275 water:IL ratio, increasing alkyl chain length of the IL cation could also cause small
276 increases in $\delta_{H(2)}$, $\delta_{H(4)}$ and $\delta_{H(5)}$ of water:IL mixtures.

277

278 **4. General discussion**

279 The effect of the cationic moiety of IL and water:IL ratio on the phase transitions of
280 starch in the water:IL mixtures was investigated. The mechanism for changes of phase
281 transitions in different solvent systems was revealed from the viewpoint of water
282 availability for starch gelatinization, interactions between water and IL, and viscosity
283 of the water:IL mixtures. From the results of FTIR and ^{1}H NMR spectra, we can
284 conclude that with increasing concentration of IL in water:IL mixtures, the
285 interactions between water and IL increased initially and then decreased (the blue shift
286 for –OH increased and then decreased in Figure 4), and that the interactions between

287 cations and anions increased (the gradual downfield movement of $\delta_{H(2)}$, $\delta_{H(4)}$ and $\delta_{H(5)}$
288 in Figure 5). FTIR results also showed that with increasing alkyl chain length of the
289 IL cation, the interactions between water and the IL increased.
290
291 In pure water, starch molecules interact with free water during heating, leading to the
292 disruption of starch crystalline and granule structures. With an increasing amount of
293 IL in water (35:1 to 10:1 water:IL ratio), the interactions between water and IL
294 increased, resulting in decreasing water availability for starch gelatinization, and in
295 turn increasing transition temperatures and enthalpy change. With a further increase of
296 IL in water (5:1 water:IL ratio), the interactions between water and IL decreased,
297 leading to increased water availability for gelatinization and decreased temperatures
298 and enthalpy change of gelatinization endotherm. Meanwhile, there were abundant IL
299 that could penetrate into starch granules with the assistance of water (with a lower
300 viscosity than for the case at 2:1 water:IL ratio) and interact with starch hydroxyls
301 (which mostly like to occur initially in amorphous regions), leading to a small
302 exothermic transition. At this water:IL ratio, the gelatinization may still be not as easy
303 as in pure water due to the limited amount of water available for this process and to
304 the higher viscosity (compared to the viscosity at higher water:IL ratios) limiting the
305 access of water to starch. As a result, the gelatinization temperatures were still higher
306 than those for starch in water. When the water:IL ratio was further decreased to 2:1,
307 the large amount of IL allowed the predominant interactions occurring between starch
308 and IL, leading to heat release of starch gelatinization (exothermic event) (Xiang et al.,

2018). In this case, although the viscosity became much higher, a higher temperature could still facilitate the starch-IL interactions.

At the same water:IL ratio (35:1, 15:1, 10:1 and 5:1), increasing alkyl chain length of the cation led to decreased thermal transition temperatures and enthalpy change of starch. The hydrophobicity of ILs increases with increasing cationic alkyl chain length (Pinkert et al., 2009), resulting in increasing interaction of ILs and water availability for starch gelatinization, thus decreasing the transition temperatures and enthalpy change of starch. At lower water:IL ratio 2:1, although the availability of IL is greater, the much higher viscosity of the water:[C_4mim][Cl] mixtures would make the interactions between IL and starch less easy and result in higher exothermic transition temperatures. In contrast, the lower viscosity of the water:[C_3mim] and water:[C_2mim][Cl] would allow them to interact with starch more easily, leading to a shift of the exothermic transition to lower temperatures.

5. Conclusions

This research shows that the phase transition behavior of maize starch in aqueous ILs is affected greatly by the water:IL ratio and the length of the cation alkyl chain. For each type of ILs, the phase transition of starch shifted to higher temperatures with decreasing water:IL ratio to 10:1. At 5:1 water:IL ratio, an exothermic transition at lower temperatures followed by an endothermic event was observed; and at 2:1 water:IL ratio, only an exothermic transition occurred. [C_4mim][Cl], which has a long

cationic alkyl chain, facilitated starch gelatinization at water:IL ratios of 35:1, 15:1, 10:1 and 5:1. In contrast, [C_3mim][Cl] and [C_2mim][Cl] with a shorter cationic alkyl chain favored the starch gelatinization at water:IL ratios of 2:1. Our results clearly showed that the phase transition of starch in water:IL mixtures is affected by the water:IL ratio and alkyl chain length of cations, which determines the interactions between water and ILs and the viscosity of water:IL mixtures. Our findings would not only increase the understanding of the mechanism of starch phase transition in water:IL mixtures, but also benefit the development of starch-based materials with desirable functional properties.

Acknowledgments

The authors gratefully acknowledge the financial support from the National Natural Science Foundation of China (31871796) and Natural Science Foundation of Tianjin City (17JCJQJC45600).

Notes

The authors declare no competing financial interest.

353 **References**

354 Cammarata, L., Kazarian, S.G., Salter, P.A., Welton, T., 2001. Molecular states of
355 water in room temperature ionic liquids. Phys. Chem. Chem. Phys. 3, 5192–5200.
356 https://doi.org/10.1039/b106900d
357 Chen, Y., Cao, Y., Zhang, Y., Mu, T., 2014. Hydrogen bonding between
358 acetate-based ionic liquids and water: Three types of IR absorption peaks and
359 NMR chemical shifts change upon dilution. J. Mol. Struct. 1058, 244–251.
360 https://doi.org/10.1016/j.molstruc.2013.11.010
361 Debet, M.R., Gidley, M.J., 2007. Why do gelatinized starch granules not dissolve
362 completely? Roles for amylose, protein, and lipid in granule "ghost" integrity. J.
363 Agric. Food Chem. 55, 4752–4760. https://doi.org/10.1021/jf070004o
364 Decaen, P., Rolland-Sabaté, A., Guilois, S., Jury, V., Allanic, N., Colomines, G.,
365 Lourdin, D., Leroy, E., 2017. Choline chloride vs choline ionic liquids for starch
366 thermoplasticization. Carbohydr. Polym. 177, 424–432.
367 https://doi.org/10.1016/j.carbpol.2017.09.012
368 Egorova, K.S., Gordeev, E.G., Ananikov, V.P., 2017. Biological activity of ionic
369 liquids and their application in pharmaceutics and medicine. Chem. Rev. 117,
370 7132–7189. https://doi.org/10.1021/acs.chemrev.6b00562
371 Hall, C.A., Le, K.A., Rudaz, C., Radhi, A., Lovell, C.S., Damion, R.A., Budtova, T.,
372 Ries, M.E., 2012. Macroscopic and microscopic study of
373 1-ethyl-3-methyl-imidazolium acetate−water mixtures. J. Phys. Chem. B 116,
374 12810–12818. https://doi.org/10.1021/jp306829c

375 Jenkins, P.J., Donald, A.M., 1998. Gelatinisation of starch: A combined
376 SAXS/WAXS/DSC and SANS study. Carbohydr. Res. 308, 133–147.
377 https://doi.org/10.1016/S0008-6215(98)00079-2
378 Lappalainen, K., Kärkkäinen, J., Lajunen, M., 2013. Dissolution and
379 depolymerization of barley starch in selected ionic liquids. Carbohydr. Polym. 93,
380 89–94. https://doi.org/10.1016/j.carbpol.2012.04.011
381 Liu, W., Budtova, T., 2013. Dissolution of unmodified waxy starch in ionic liquid and
382 solution rheological properties. Carbohydr. Polym. 93, 199–206.
383 https://doi.org/10.1016/j.carbpol.2012.01.090
384 Liu, Y., Yu, J., Copeland, L., Wang, S., Wang, S., 2019. Gelatinization behavior of
385 starch: Reflecting beyond the endotherm measured by differential scanning
386 calorimetry. Food Chem. 284, 53–59.
387 https://doi.org/10.1016/j.foodchem.2019.01.095
388 Lu, B., Xu, A., Wang, J., 2014. Cation does matter: How cationic structure affects the
389 dissolution of cellulose in ionic liquids. Green Chem. 16, 1326–1335.
390 https://doi.org/10.1039/c3gc41733f
391 Mahmood, H., Moniruzzaman, M., Yusup, S., Muhammad, N., Iqbal, T., Akil, H.M.,
392 2017a. Ionic liquids pretreatment for fabrication of agro-residue/thermoplastic
393 starch based composites: A comparative study with other pretreatment
394 technologies. J. Clean. Prod. 161, 257–266.
395 https://doi.org/10.1016/j.jclepro.2017.05.110
396 Mahmood, H., Moniruzzaman, M., Yusup, S., Welton, T., 2017b. Ionic liquids

assisted processing of renewable resources for the fabrication of biodegradable composite materials. Green Chem. 19, 2051–2075. https://doi.org/10.1039/c7gc00318h

Mäki-Arvela, P., Anugwom, I., Virtanen, P., Sjöholm, R., Mikkola, J.P., 2010. Dissolution of lignocellulosic materials and its constituents using ionic liquids-A review. Ind. Crops Prod. 32, 175–201. https://doi.org/10.1016/j.indcrop.2010.04.005

Mateyawa, S., Xie, D.F., Truss, R.W., Halley, P.J., Nicholson, T.M., Shamshina, J.L., Rogers, R.D., Boehm, M.W., McNally, T., 2013. Effect of the ionic liquid 1-ethyl-3-methylimidazolium acetate on the phase transition of starch: Dissolution or gelatinization? Carbohydr. Polym. 94, 520–530. https://doi.org/10.1016/j.carbpol.2013.01.024

Mekonnen, T., Mussone, P., Khalil, H., Bressler, D., 2013. Progress in bio-based plastics and plasticizing modifications. J. Mater. Chem. A 1, 13379–13398. https://doi.org/10.1039/c3ta12555f

Ning, W., Xingxiang, Z., Haihui, L., Benqiao, H., 2009. 1-Allyl-3-methylimidazolium chloride plasticized-corn starch as solid biopolymer electrolytes. Carbohydr. Polym. 76, 482–484. https://doi.org/10.1016/j.carbpol.2008.11.005

Papanyan, Z., Roth, C., Wittler, K., Reimann, S., Ludwig, R., 2013. The dissolution of polyols in salt solutions and ionic liquids at molecular level: Ions, counter ions, and hofmeister effects. ChemPhysChem 14, 3667–3671. https://doi.org/10.1002/cphc.201300465

Pinkert, A., Marsh, K.N., Pang, S., Staiger, M.P., 2009. Ionic liquids and their interaction with cellulose. Chem. Rev. 109, 6712–6728. https://doi.org/10.1002/chin.201017232

Ramesh, S., Liew, C.W., Arof, A.K., 2011. Ion conducting corn starch biopolymer electrolytes doped with ionic liquid 1-butyl-3-methylimidazolium hexafluorophosphate. J. Non. Cryst. Solids 357, 3654–3660. https://doi.org/10.1016/j.jnoncrysol.2011.06.030

Ratnayake, W.S., Otani, C., Jackson, D.S., 2009. DSC enthalpic transitions during starch gelatinisation in excess water, dilute sodium chloride and dilute sucrose solutions. J. Sci. Food Agric. 89, 2156–2164. https://doi.org/10.1002/jsfa.3709

Ren, F., Wang, J., Yu, J., Xiang, F., Wang, S., Wang, S., Copeland, L., 2019. Dissolution of maize starch in aqueous ionic liquid: the role of alkyl chain length of cation and ratio of water:ionic liquid. ACS Sustain. Chem. Eng. 7, 2898–6905. https://doi.org/10.1021/acssuschemeng.8b06432

Sankri, A., Arhaliass, A., Dez, I., Gaumont, A.C., Grohens, Y., Lourdin, D., Pillin, I., Rolland-Sabaté, A., Leroy, E., 2010. Thermoplastic starch plasticized by an ionic liquid. Carbohydr. Polym. 82, 256–263. https://doi.org/10.1016/j.carbpol.2010.04.032

Sciarini, L.S., Rolland-Sabaté, A., Guilois, S., Decaen, P., Leroy, E., Le Bail, P., 2015. Understanding the destructuration of starch in water-ionic liquid mixtures. Green Chem. 17, 291–299. https://doi.org/10.1039/c4gc01248h

Shogren, R.L., Fanta, G.F., Doane, W.M., 1993. Development of starch based plastics

441 - A reexamination of selected polymer systems in historical perspective. Starch -
442 Stärke 45, 276–280. https://doi.org/10.1002/star.19930450806
443 Vicent-Luna, J.M., Romero-Enrique, J.M., Calero, S., Anta, J.A., 2017. Micelle
444 formation in aqueous solutions of room temperature ionic liquids: A molecular
445 dynamics study. J. Phys. Chem. B 121, 8348–8358.
446 https://doi.org/10.1021/acs.jpcb.7b05552
447 Wilpiszewska, K., Spychaj, T., 2011. Ionic liquids: Media for starch dissolution,
448 plasticization and modification. Carbohydr. Polym. 86, 424–428.
449 https://doi.org/10.1016/j.carbpol.2011.06.001
450 Xiang, F., Copeland, L., Wang, S., Wang, S., 2018. Nature of phase transitions of
451 waxy maize starch in water-ionic liquid mixtures. Int. J. Biol. Macromol. 112,
452 315–325. https://doi.org/10.1016/j.ijbiomac.2018.01.158
453 Xie, F., Flanagan, B.M., Li, M., Truss, R.W., Halley, P.J., Gidley, M.J., McNally, T.,
454 Shamshina, J.L., Rogers, R.D., 2015. Characteristics of starch-based films with
455 different amylose contents plasticised by 1-ethyl-3-methylimidazolium acetate.
456 Carbohydr. Polym. 122, 160–168. https://doi.org/10.1016/j.carbpol.2014.12.072
457 Xu, A., Cao, L., Wang, B., 2015a. Facile cellulose dissolution without heating in
458 [C4mim][CH3COO]/DMF solvent. Carbohydr. Polym. 125, 249–254.
459 https://doi.org/10.1016/j.carbpol.2015.02.045
460 Xu, A., Chen, L., Wang, J., 2018. Functionalized imidazalium carboxylates for
461 enhancing practical applicability in cellulose processing. Macromolecules 51,
462 4158–4166. https://doi.org/10.1021/acs.macromol.8b00724

Xu, A., Guo, X., Xu, R., 2015b. Understanding the dissolution of cellulose in 1-butyl-3-methylimidazolium acetate+DMAc solvent. Int. J. Biol. Macromol. 81, 1000–1004. https://doi.org/10.1016/j.ijbiomac.2015.09.058

Xu, A., Guo, X., Zhang, Y., Li, Z., Wang, J., 2017. Efficient and sustainable solvents for lignin dissolution: Aqueous choline carboxylate solutions. Green Chem. 19, 4067–4073. https://doi.org/10.1039/c7gc01886j

Zhang, B., Chen, L., Xie, F., Li, X., Truss, R.W., Halley, P.J., Shamshina, J.L., Rogers, R.D., McNally, T., 2015. Understanding the structural disorganization of starch in water-ionic liquid solutions. Phys. Chem. Chem. Phys. 17, 13860–13871. https://doi.org/10.1039/c5cp01176k

Zhang, B., Xie, F., Shamshina, J.L., Rogers, R.D., McNally, T., Halley, P.J., Truss, R.W., Chen, L., Zhao, S., 2017a. Dissolution of starch with aqueous ionic liquid under ambient conditions. ACS Sustain. Chem. Eng. 5, 3737–3741. https://doi.org/10.1021/acssuschemeng.7b00784

Zhang, B., Xie, F., Shamshina, J.L., Rogers, R.D., McNally, T., Wang, D.K., Halley, P.J., Truss, R.W., Zhao, S., Chen, L., 2017b. Facile preparation of starch-based electroconductive films with ionic liquid. ACS Sustain. Chem. Eng. 5, 5457–5467. https://doi.org/10.1021/acssuschemeng.7b00788

Zhang, S., Wang, C., Fu, X., Liu, H., Yu, L., Qiao, Q., Jiang, T., 2016. A comparison study on phase transition and structure of cornstarch in dimethyl sulfoxide and ionic liquid systems. J. Cereal Sci. 71, 53–60. https://doi.org/10.1016/j.jcs.2016.07.016

Zhao, D., Wang, C., Luo, X., Fu, X., Liu, H., Yu, L., 2015. Morphology and phase transition of waxy cornstarch in solvents of 1-allyl-3-methylimidazolium chloride/water. Int. J. Biol. Macromol. 78, 304–312. https://doi.org/10.1016/j.ijbiomac.2015.04.020

Zhu, S., Wu, Y., Chen, Q., Yu, Z., Wang, C., Jin, S., Ding, Y., Wu, G., 2006. Dissolution of cellulose with ionic liquids and its application: A mini-review. Green Chem. 8, 325–327. https://doi.org/10.1039/b601395c

Figure captions

Figure 1. Structures of the ionic liquids used.

Figure 2. DSC thermograms of maize starch in different water:IL mixtures. Water:[C_4mim][Cl]-MS, solid line; Water:[C_3mim][Cl]-MS, dot line; Water:[C_2mim][Cl]-MS, dash-dot line. C2, C3, and C4 indicate the alkyl chain length of cation of ILs.

Figure 3. Normal light (NL) and polarized light (PL) microscopic images of native starch at T_o, T_p and T_c in different water:IL mixtures. The scale of images was 20 μm. (a) Native maize starch; (b) Pure water-MS, (c) Water:[C_4mim][Cl]-15:1-MS, (d) Water:[C_4mim][Cl]-5:1-MS, (e) Water:[C_4mim][Cl]-2:1-MS.

Figure 4. ATR-FTIR spectra of pure water and water:IL mixtures at different molar ratios of water:IL.

Figure 5. ^{1}H-NMR spectra of water:IL mixtures at different molar ratios of water:IL.

Figure 1

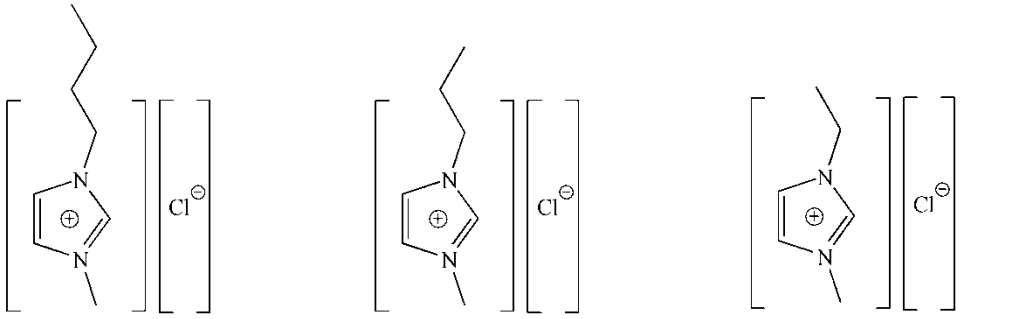

1-butyl-3-methylimidazolium chloride [C_4mim][Cl]

1-propyl-3-methylimidazolium chloride [C_3mim][Cl]

1-ethyl-3-methylimidazolium chloride ([C_2mim][Cl])

Figure 2

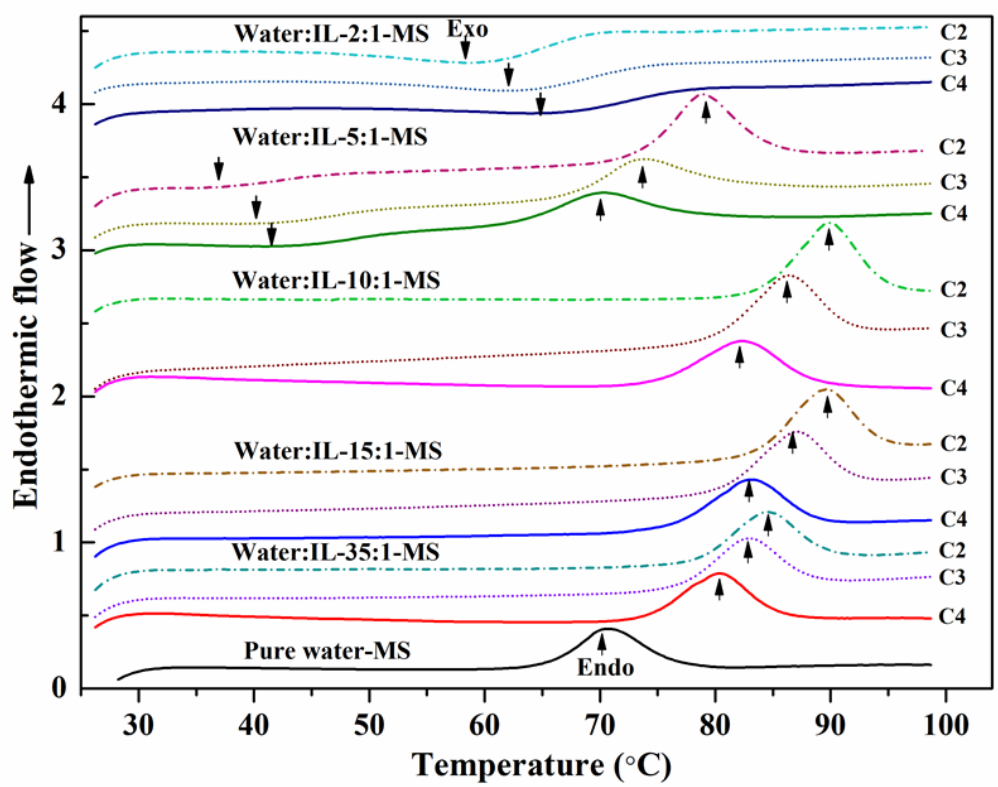
Water:IL-2:1-MS
Exo
C2
C3
C4
Water:IL-5:1-MS
C2
C3
C4
Water:IL-10:1-MS
C2
C3
C4
Water:IL-15:1-MS
C2
C3
C4
Water:IL-35:1-MS
C2
C3
C4
Pure water-MS
Endo
Endothermic flow
Temperature (°C)
0
1
2
3
4
30
40
50
60
70
80
90
100

Figure 3

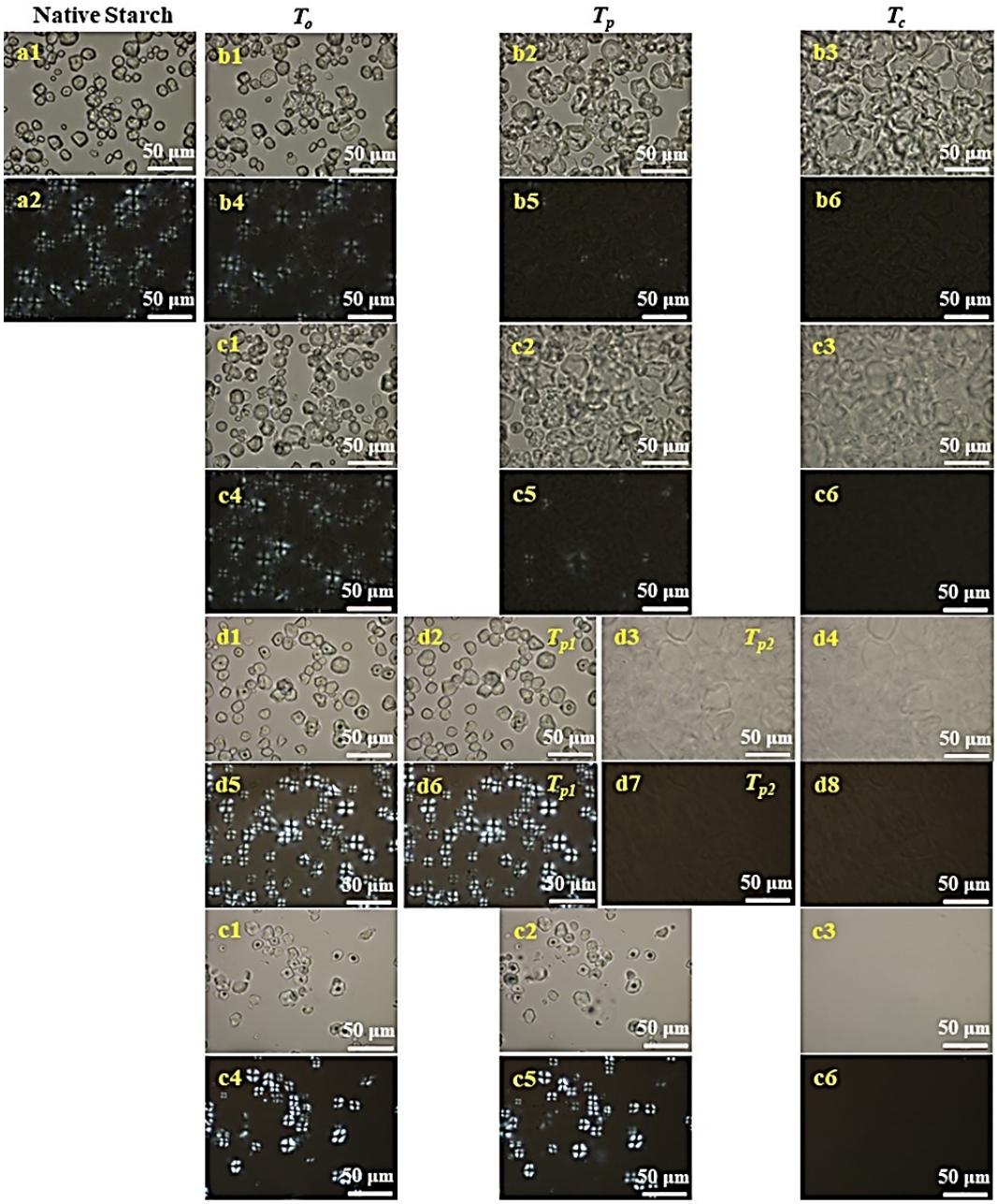
Native Starch
T_o
T_p
T_c
a1
a2
b1
b2
b3
b4
b5
b6
c1
c2
c3
c4
c5
c6
d1
d2
T_{p1}
d3
T_{p2}
d4
d5
d6
T_{p1}
d7
T_{p2}
d8
c1
c2
c3
c4
c5
c6
50 μm

Figure 4

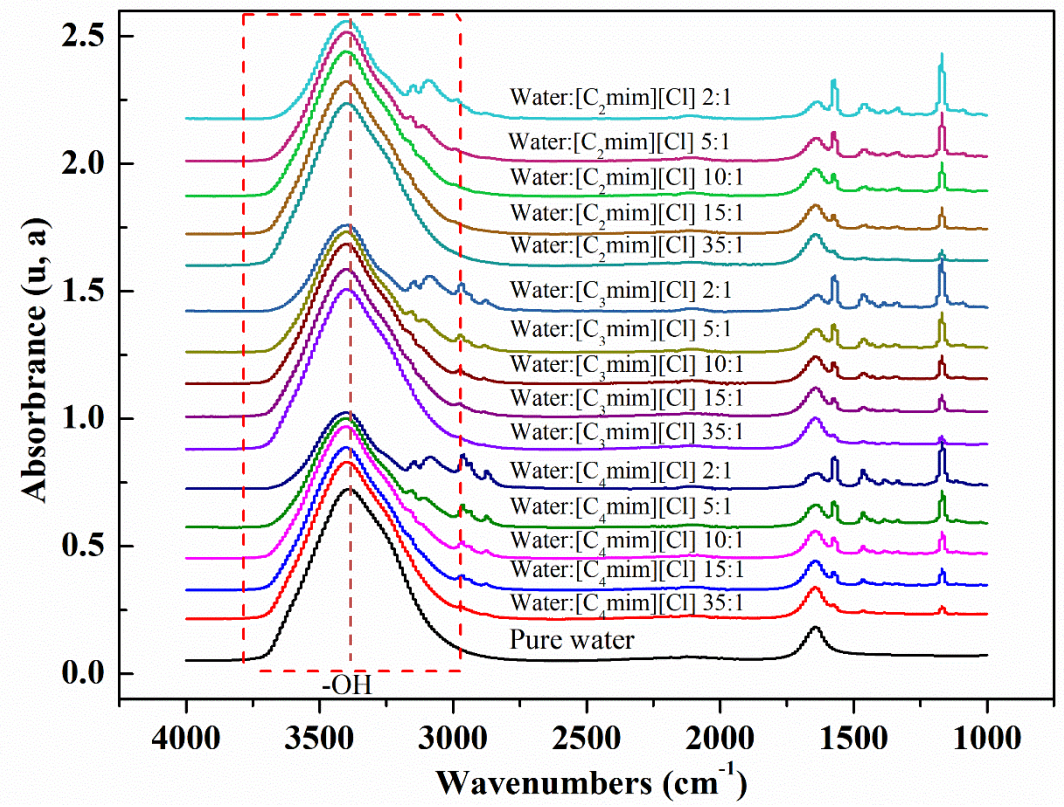
Absorbrance (u, a)
Wavenumbers (cm-1)
-OH
Water:[C2mim][Cl] 2:1
Water:[C2mim][Cl] 5:1
Water:[C2mim][Cl] 10:1
Water:[C2mim][Cl] 15:1
Water:[C2mim][Cl] 35:1
Water:[C3mim][Cl] 2:1
Water:[C3mim][Cl] 5:1
Water:[C3mim][Cl] 10:1
Water:[C3mim][Cl] 15:1
Water:[C3mim][Cl] 35:1
Water:[C4mim][Cl] 2:1
Water:[C4mim][Cl] 5:1
Water:[C4mim][Cl] 10:1
Water:[C4mim][Cl] 15:1
Water:[C4mim][Cl] 35:1
Pure water

Figure 5

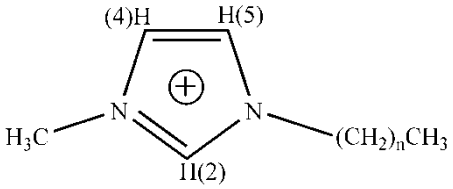
(4)H
H(5)
N
N
H3C
(CH2)nCH3
H(2)

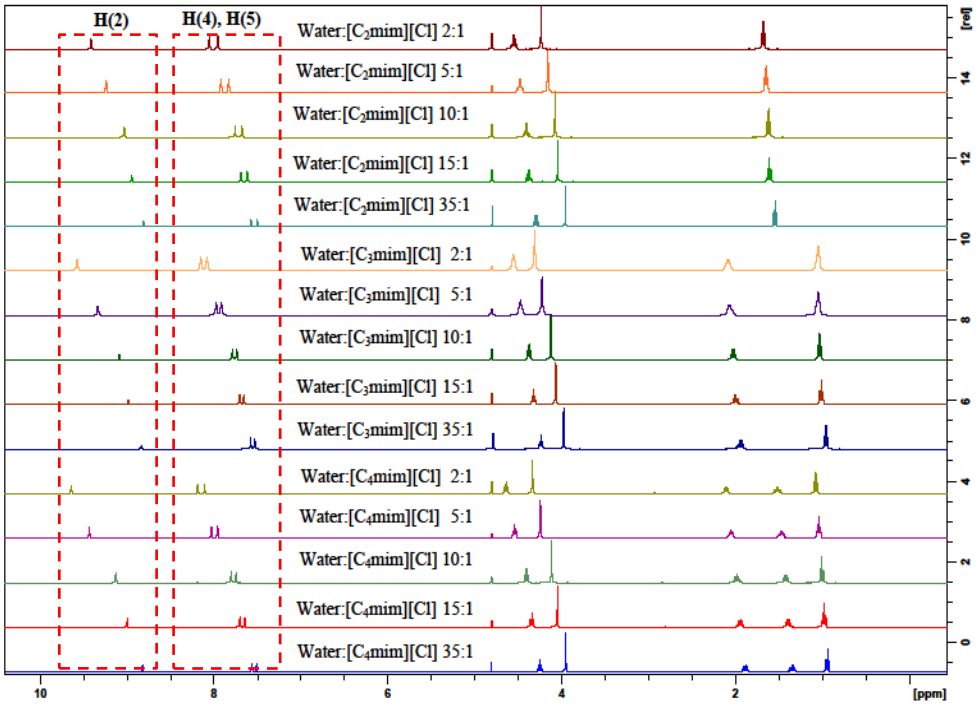
H(2)
H(4), H(5)
Water:[C2mim][Cl] 2:1
Water:[C2mim][Cl] 5:1
Water:[C2mim][Cl] 10:1
Water:[C2mim][Cl] 15:1
Water:[C2mim][Cl] 35:1
Water:[C3mim][Cl] 2:1
Water:[C3mim][Cl] 5:1
Water:[C3mim][Cl] 10:1
Water:[C3mim][Cl] 15:1
Water:[C3mim][Cl] 35:1
Water:[C4mim][Cl] 2:1
Water:[C4mim][Cl] 5:1
Water:[C4mim][Cl] 10:1
Water:[C4mim][Cl] 15:1
Water:[C4mim][Cl] 35:1
10
8
6
4
2
[ppm]
[rel]

Table 1. DSC results of maize starch in different water:IL mixtures.

Samples	Transition	T_o (°C)	T_P (°C)	T_c (°C)	ΔH (J/g)
Pure water-MS	Endo	65.8 ± 0.2^{g}	70.8 ± 0.2^{d}	76.9 ± 0.2^{c}	11.4 ± 0.3^{a}
Water:[C_4mim][Cl]-35:1-MS	Endo	74.0 ± 0.2^{h}	80.2 ± 0.1^{e}	85.2 ± 0.1^{e}	12.9 ± 0.2^{b}
Water:[C_4mim][Cl]-15:1-MS	Endo	76.5 ± 0.1^{ij}	83.2 ± 0.2^{g}	88.6 ± 0.0^{g}	15.1 ± 0.1^{c}
Water:[C_4mim][Cl]-10:1-MS	Endo	75.2 ± 0.4^{hi}	82.1 ± 0.3^{f}	88.1 ± 0.3^{fg}	15.5 ± 0.5^{cd}
Water:[C_4mim][Cl]-5:1-MS	Exo → Endo	33.1 ± 0.5^{c}	T_{p1} 43.5 ± 0.4 → T_{p2} 70.0 ± 0.1	76.8 ± 0.1^{c}	12.7 ± 0.2^{b}
Water:[C_4mim][Cl]-2:1-MS	Exo	58.5 ± 0.4^{f}	63.7 ± 0.2^{c}	77.0 ± 0.3^{c}	-5.7 ± 0.1^{C}
Water:[C_3mim][Cl]-35:1-MS	Endo	76.9 ± 0.2^{j}	82.8 ± 0.1^{g}	88.0 ± 0.3^{f}	13.2 ± 0.1^{b}
Water:[C_3mim][Cl]-15:1-MS	Endo	80.6 ± 0.2	87.1 ± 0.1^{i}	92.0 ± 0.1^{i}	15.7 ± 0.2^{d}
Water:[C_3mim][Cl]-10:1-MS	Endo	80.0 ± 0.2^{kl}	86.5 ± 0.1^{i}	91.6 ± 0.1^{i}	17.5 ± 0.0^{f}
Water:[C_3mim][Cl]-5:1-MS	Exo → Endo	30.6 ± 0.4^{b}	T_{p1} 41.4 ± 0.3 → T_{p2} 73.5 ± 0.2	80.5 ± 0.3^{d}	15.3 ± 0.2^{b}
Water:[C_3mim][Cl]-2:1-MS	Exo	51.3 ± 0.1^{e}	61.6 ± 0.4^{b}	73.7 ± 0.3^{b}	-9.5 ± 0.2^{B}
Water:[C_2mim][Cl]-35:1-MS	Endo	78.6 ± 0.1^{k}	84.5 ± 0.2^{h}	89.6 ± 0.1^{h}	13.4 ± 0.1^{b}
Water:[C_2mim][Cl]-15:1-MS	Endo	84.0 ± 0.1^{m}	90.0 ± 0.2^{j}	94.1 ± 0.1^{k}	16.2 ± 0.1^{e}
Water:[C_2mim][Cl]-10:1-MS	Endo	83.7 ± 0.1^{m}	89.4 ± 0.1^{j}	93.5 ± 0.1^{j}	18.7 ± 0.3^{g}
Water:[C_2mim][Cl]-5:1-MS	Exo → Endo	29.1 ± 0.2^{a}	T_{p1} 37.3 ± 0.3 → T_{p2} 78.4 ± 0.3	85.1 ± 0.2^{e}	18.1 ± 0.1^{f}
Water:[C_2mim][Cl]-2:1-MS	Exo	48.0 ± 0.5^{d}	57.8 ± 0.1^{a}	67.9 ± 0.1^{a}	-10.5 ± 0.2^{A}

Values are means ± standard deviation. Values with the same lowercase letters in the same column are not significantly different ($p < 0.05$).

Values with the same uppercase letters in the same column for the exothermic transition are not significantly different ($p < 0.05$).

595 **Table 2.** Viscosity, wavenumbers (-OH of water) and chemical shift ($\delta_{H(2)}$, $\delta_{H(4)}$ and
596 $\delta_{H(5)}$ of cation imidazolium ring) of water:IL mixtures at different molar ratios.

Samples	Viscosity (mPa·s)	Wavenumbers (cm^{-1})	Chemical shift (ppm)		
		─OH	$\delta_{H(2)}$	$\delta_{H(4)}$	$\delta_{H(5)}$
Pure water	0.81 ± 0.01[a]	3388.94	N.D.	N.D.	N.D.
Water:[C_4mim][Cl] 35:1	1.40 ± 0.01[d]	3400.27	8.82	7.58	7.52
Water:[C_4mim][Cl] 15:1	2.34 ± 0.02[g]	3400.92	9.03	7.72	7.67
Water:[C_4mim][Cl] 10:1	3.45 ± 0.03[j]	3404.14	9.12	7.80	7.75
Water:[C_4mim][Cl] 5:1	8.42 ± 0.01[m]	3400.87	9.44	8.03	7.96
Water:[C_4mim][Cl] 2:1	32.86 ± 0.02[p]	3400.63	9.64	8.18	8.10
Water:[C_3mim][Cl] 35:1	1.33 ± 0.02[c]	3397.30	8.80	7.56	7.50
Water:[C_3mim][Cl] 15:1	2.18 ± 0.01[f]	3400.55	8.98	7.70	7.64
Water:[C_3mim][Cl] 10:1	3.10 ± 0.01[i]	3401.05	9.09	7.78	7.73
Water:[C_3mim][Cl] 5:1	6.11 ± 0.02[l]	3396.59	9.34	7.98	7.92
Water:[C_3mim][Cl] 2:1	19.03 ± 0.02[o]	3396.36	9.57	8.15	8.08
Water:[C_2mim][Cl] 35:1	1.24 ± 0.02[b]	3397.03	8.76	7.53	7.49
Water:[C_2mim][Cl] 15:1	1.93 ± 0.01[e]	3398.56	8.95	7.69	7.62
Water:[C_2mim][Cl] 10:1	2.63 ± 0.01[h]	3399.72	9.03	7.76	7.67
Water:[C_2mim][Cl] 5:1	5.85 ± 0.01[k]	3395.76	9.24	7.91	7.83
Water:[C_2mim][Cl] 2:1	17.05 ± 0.02[n]	3395.53	9.42	8.05	7.96

597 Values are means ± standard deviation. Values with the same lowercase letters in the
598 same column are not significantly different ($p < 0.05$).

599